Spinetti *et al*.

MicroRNA-15a and microRNA-16 Impair Human Circulating Pro-Angiogenic Cell (PAC) Functions and are increased in the PACs and Serum of Patients with Critical Limb Ischemia

Online Supplements

Detailed Methods

Clinical study

ClinicalTrials.gov: NCT01269580, Title: Diabetic Foot and Vascular Progenitor Cells. The study was conducted on patients with critical limb ischemia (CLI) with or without type 2 diabetes mellitus (T2D) enrolled at the time of percutaneous angioplasty (PTA) for CLI. CLI was defined according to TASC criteria (2007). Exclusion criteria were drug-induced diabetes, liver failure or dialysis due to renal failure, cancer, chemotherapic treatment, pregnancy, lack of consent to participate to the study. CLI patients were visited at a 12 month follow up to monitor for the occurrence of selected events (i.e. mortality, major amputation, and restenosis in treated limb). The primary endpoint of the trial is defining the potential prognostic value of the altered number and migratory ability of antigenically characterized PACs for the evolution of major cardiovascular endpoints at 12 month follow up (June 2012). The main results of the study will be the subject of a separate manuscript.

miR transfection

PACs were transfected with 50 nmol/L pre-miR mimics (pre-miR-15a and pre-miR-16) or with 50 nmol/L miR inhibitors (anti-miR-15a and anti-miR-16), or negative control (a non-targeting sequence, also identified as scramble, SCR, throughout the manuscript) (all from Applied Biosystems) using GeneSilencer (Dharmacon) following the manufacturer's instructions. Using the same protocol, vascular smooth muscle cells (VSMCs) were transfected with 50 nmol/L pre-miR-15a or SCR. When pre- or anti-miR15a and -16 were transfected together in PACs, 25 nmol/L each was used to reach the final 50 nmol/L concentration. Mimic and inhibitor concentrations were selected based on pilot concentration-response experiments, in which the changes in relative miR-15a and -16 expression were measured by TaqMan PCR (*vide infra*). In parallel experiments, we assessed the efficiency of PAC transfection by transfecting fluorescently-labeled miR-mimic (miR-mimic-Pe-Cy3) (Applied Biosystems). The percentage of transfected PACs was greater than 95%.

Cell culture

To prepare PACs, PB (35ml) was withdrawn from forearm vein puncture and MNCs were separated on Ficoll-Paque PLUS (Amersham Biosciences) gradient at 400g. To ensure PACs enrichment, MNCs ($1x10^7$/well) were plated on fibronectin (Sigma)-coated 6-well plates (BD Falcon) and cultured in EBM-2, supplemented with EGM-2 MV SingleQuots and 10% FBS (all from Cambrex) for 4 days. Pericyetes were prepared from human vena saphena as previously described[1]; human vascular smooth muscle cells (VSMCs), human umbilical vein endothelial cells (HUVECs), human microvascular ECs (HMVECs), human coronary artery EC (HCAECs) and human aorta ECs (HAECs) were all purchased by Lonza and cultured accordingly to Lonza protocols.

Exosome isolation

Cell conditioned medium (CCM) or plasma were processed for exosome collection and ultrapurification, as described[2]. For CCM, cells were removed by centrifugation (500*g*, 5 min), then CCM or plasma were clarified by centrifugation (2000*g*, 30 min followed by 12000*g*, 45 min at 4°C). Exosomes were collected by ultracentrifugation (110000*g*, 2 hours),

washed in PBS and pelleted. The purified exosome fraction was re-suspended in PBS for use. Exosome purity was confirmed by flow cytometric analysis. Briefly, exosomes were conjugated to 4μm latex beads/aldehyde sulphate for easy detection as described previously[3]. Exosome-coupled beads were washed in PBS/BSA 0.5%, stained with AnnexinV (FITC) and anti-CD63 (APC) as exosomes markers for 15min at room temperature. Stained beads-conjugated exosomes were analyzed in a FACSCanto flow cytometer using the FACSDiva software (both from BD Biosciences).

RNA extraction and TaqMan quantitative Real Time PCR

RNA was extracted from cultured cells using TRIzol reagent (Invitrogen) following the manufacturer's instructions. The concentration of total RNA was determined using the Nanodrop ND1000 Spectrophotometer (Thermo Scientific) and the size and integrity of RNAs was assessed using an Agilent 2100 Bioanalyzer (Agilent Technologies).

For serum and plasma analyses, 10 mL of peripheral venous blood was collected. Half of this was placed in a citrate tube (BD) containing anticoagulants. The remainder was kept in plain tubes without an anticoagulant. 'Whole plasma' was obtained by centrifugation of the citrated blood (1500 rpm, 15 min, 4°C). Some of this plasma (1 mL) underwent a second centrifugation (14000 rpm, 15 min, 4°C) to form a platelet pellet. The top 850 μL was removed ('platelet-poor plasma') and the remaining fraction (including the platelet pellet) was also saved ('platelet-enriched plasma'). Serum was collected by allowing the blood in the plain tube to coagulate at room temperature for 30 min, followed by centrifugation (1500 rpm, 15 min, 4°C). RNA was extracted using 100 μl of input fluid and the miRNeasy kit (Qiagen), with 25 fmol of the synthetic C.elegans-miR-39 (cel-39) spiked-in as a normalizer, as described by Kroh E *et al*. 2010[4].

Argonaute-2 (Ago-2) immunoprecipitation from whole plasma was performed using the method described above by Arroyo *et al*[5]. In brief, a monoclonal antibody to Ago-2 (Abcam) (or non-immune mouse IgG as control) was conjugated with magnetic anti-mouse IgG beads. A 1:1 dilution of plasma and PBS (100 μL each) was incubated with the conjugated antibody at 4°C overnight. Following this, the beads were washed and the RNA extracted as described above.

RNA reverse transcription to measure miRs was performed with the TaqMan miR reverse transcription kit following the manufacturer's instructions (Applied Biosystems). miR expression was analyzed by the Applied 7900 Real Time PCR System and normalized to the U6 small nucleolar RNA (snRU6) for PACs and/or synthetic cel-miR-39 (Qiagen) for serum and plasma. For gene expression analyses, single-strand complementary DNA (cDNA) was synthesized from 1 μg of total RNA using TaqMan Reverse Transcription reagents (Applied Biosystems). Quantitative RT-PCR was performed with the Applied 7900 Real Time PCR System (Applied Biosystems) using the following primers: 18s rRNA (forward 5'-CGCAGCTAGGAATAATGGAATAGG-3'; reverse 5'-CATGGCCTCAGTTCCGAAA-3'), AKT3 (forward: 5'-GCAGAGGCAAGAAGAGGAGA-3'; reverse: 5'-ACTTGCCTTCTCTCGAACCA-3'), FGFR1 (forward 5'-CCTCTATGTGGGCATGGTTT-3'; reverse 5' TACAGGAAGGACGATCTGGG-3'), VEGF-A (forward: 5'-CCCACTGAGGAGTCCAACAT-3'; reverse: 5'-AAATGCTTTCTCCGCTCTGA-3'), CXCR4 (forward: 5'-GGTGGTCTATGTTGGCGTCT-3'; reverse: 5'-TGGAGTGTGACAGCTTGGAG-3'); KDR (forward: 5'-GTGACCAACATGGAGTCGTG-3'; reverse: 5'-TGCTTCACAGAAGACCATGC-3').3') Dicer (forward: 5'-ACCAAGTTGCATTTCGGTAT-3', reverse: 5'-AGGAAATTTCGAGCACATGA-3'), Drosha (forward: 5'-CACCTGTTCTAGCAGCTCAGAC-3', reverse: 5'-CTCCTCCCACTGAAGCATATTG-3'), Pri-mir15a-16-1 (forward: 5'-AAGGTGCAGGCCATATTGTG-3', reverse: 5'- AAGGCACTGCTGACATTGC-3'). Data were normalized to 18S ribosomal RNA as an endogenous control.

For both miR and gene expression, each PCR reaction was performed in triplicate and analyzes were performed by either the 2–ddCt method[6, 7] or after obtaining relative miR abundance, using a standard curve built on serial dilutions of synthetic mature double-stranded miR templates (Ambion). In the latter case, data were expressed as mean relative

quantity versus internal control (namely snU6 for cells and exosomes or cel-miR-39 for serum and plasma). Concentrations of each miR were calculated from the standard curve linear regression line using the following formula: $10^{-(\text{Ct-Y intercept})/\text{slope value})}$, where Ct represents the threshold cycle value[8, 9]. Values were then normalized to internal control using [miR]/[control].

Luciferase assays

To investigate whether VEGF-A, and AKT-3 are direct targets of miR-15a and miR-16, the 3'-UTR of the potentials target genes were inserted downstream of a luciferase open reading frame (pLUC). VEGF-A 3'-UTR (SC217121) vector was purchased from Origene and AKT3 3'-UTR (S811011) from SwitchGear Genomics.

Conserved binding sites in VEGF-A and AKT-3 3'UTR were identified using TargetScan 6.2 (http://www.targetscan.org). Binding sites are: VEGF-A position 292-299; AKT-3 positions 235-242 and 3041-3048. For controls, we prepared similar vectors in which five nucleotide mutations were inserted in the 3'-UTR sequences complementary to the miR-15a/16 binding sequences. For AKT-3, plasmids with a single or double mutation in the 3'-UTR were prepared. Primers for mutation are reported in **Online Table VI**. HPLC-purified oligonucleotides (Sigma) were used for mutagenesis, performed with Pfu enzyme following the *in vitro* mutagenesis kit protocol (Invitrogen). The different luciferase constructs were transfected into HEK293 cells together with pre-miR-15a or pre-miR-16 or both or a scrambled oligonucleotide sequence (control). Cells were cultured for 48 hours and assayed with the Dual-Luciferase Reporter Assay System (Promega). Values were normalized using Renilla expression level.

Western Blot analyses

PAC proteins were extracted by incubation with lysis buffer containing 50 mmol/L Hepes, 150 mmol/L NaCl, 1 mmol/L EDTA, 1 mmol/L EGTA, 25 mmol/L NaF, 5 mmol/L NaPPi, 1%Triton, 1% NP40, 1mmol/L Na_3VO_4, 0.25% sodium deoxycholate, 0.5 mmol/L Na-orthovanadate, 1 mmol/L benzamidine and 0.1 mmol/L phenylmethylsulfonyl fluoride. Thirty micrograms of protein were separated on SDS-polyacrylamide gels and transferred to polyvinylidene difluoride membranes (PVDF, GE Healthcare, Slough, UK) to be probed with the following antibodies: AKT3 and pAKT (both 1:1000), VEGF-A (1:500), KDR (1:1000), FGFR1 (1:1000), Phospo-eNOS (ser1177) (1:1000) (all from Cell Signaling), eNOS (1:1000, Santa Cruz), BCL2 (1:1000, Dako) and β-actin (1:5000, Santa Cruz Biotechnology) (used as loading control). For detection, goat anti-rabbit or goat anti-mouse secondary antibodies conjugated to horseradish peroxidase (GE Healthcare, 1:2000) were used. Detection was developed by a chemiluminescence reaction (ECL, GE Healthcare).

Flow Cytometry

PACs ($5x10^5$) were stained with appropriate fluorescent conjugated antibodies: CD34 (PE-Cy7), CD45 (APC-H7), CD14 (FITC), CXCR4 (APC) all from BD Biosciences, and KDR (PE) from R&D. After 15 min incubation at room temperature in the dark, cells were washed, resuspended in PBS and analyzed. For each test, $1x10^5$ to $5x10^5$ total events were analyzed using a FACSCanto flow cytometer with the FACSDiva software (both BD Biosciences).

Migration assay

For PACs migration assay 5 μm pore-size filter-equipped transwell chambers (Corning) coated with fibronectin were used. Cells ($7.5x10^4$) were placed in the upper chamber and allowed to migrate toward SDF-1a (R&D) (100 ng/mL), FBS (10% in EBM medium), VEGF-A (100 ng/mL), bFGF (100 ng/mL), or BSA (control) for 16 hours at 37°C. The cells on the upper part of the filter were scraped away before fixing the filter. The lower side of the filter (containing the migrated cells) was mounted with Vectashield containing DAPI. For each chamber, migrated cells were counted in 5 random fields at 20X magnification. Migration data are expressed as the number of cells migrated toward the specific chemoattractant vs. the number of cells migrated in the absence of stimulus (i.e. cells migrated to BSA).

Vascular smooth muscle cell (VSMC) migration was evaluated by scratch assay. VSMCs were transfected with premiR-15a or scramble (each at 50 nmol/L). A spatula was used to make a scratch in the cell monolayer. Cells were treated with hydroxyurea (2 mmol/L, Sigma) to arrest cell proliferation and incubated with 10% FBS/DMEM. Pictures were taken immediately after scratching and 6, 12 and 24 hours thereafter. Gap closure was quantified using captured microscopic fields (magnification 4X). Experiments were repeated 4X.

VSMC proliferation by BrdU incorporation assay

After 24 hours of transfection, VSMCs over-expressing miR-15a or scramble were seeded in a 96-well plate ($3x10^3$ cells per well) and treated for 12 hours with 0.5% FBS/DMEM. The medium was then replaced by 10% FBS/DMEM with BrdU (10 µmol/L). BrdU incorporation was measured by the BrdU ELISA assay kit (Roche) after 6, 12 and 24 hours of stimulation with high FBS. Experiments were repeated 4X.

***In vitro* angiogenesis**

Capillary-like network formation Assay: $5X10^4$ PHK67 (Sigma) stained, FITC-labelled PACs were added to 8-well chamber slides pre-coated with 150 µL Matrigel (Becton Dickinson), together with $50x10^3$ PKH26 red-stained (Sigma) HUVECs in a total volume of 150 µL EBM-2 with 0.1% BSA. After 16 hours incubation at 37°C, floating cells were removed by gentle washing and the adherent cells were fixed in 2% paraformaldehyde and treated with DAPI containing PBS. The assays were performed in duplicate wells. PACs effect on network formation from HUVECs was measured by counting the 1) number of intersection points, 2) average and total tube length, and 3) percentage of adherent PACs, in 5 microphotographs of random view fields (magnification 20X). Fluorescence was visualized and captured using an AXIO OBSERVER A1 microscope equipped with digital image processing software (AxioVision Imaging System), both from Zeiss. Similar assays were repeated adding the conditioned medium of PACs to the HUVECs.

Spheroid assay: 3D angiogenesis assay (with CCM of PACs and HUVECs) was performed according manufacturer's instructions (PromoCell).

Apoptosis assay

Apoptosis was measured by quantifying the percentage of Annexin V^{pos}/PI^{neg} PACs by flow cytometry. In brief, transfected PACs (2×10^5 cells) were stained with 5 µL of Annexin V (BD Biosciences) and 1 µL of propidium iodide (PI) in 200 µL binding buffer for 15 min at room temperature in the dark. After incubation, cells were suspended in 150 µL of Annexin Binding Buffer and the percentage of Annexin V^{pos}/PI^{neg} PACs was assessed using FACS Canto flow cytometer and FACS Diva Software (both from BD Biosciences).

ELISA

VEGF protein levels were measured in PACs conditioned to a medium level using a commercially available ELISA kit (R&D). Briefly, transfected PACs were cultured for 24 hours in EBM-2 medium in the absence of serum, then CM was harvested, centrifuged at 2000 rpm for 10 min at RT, and stored at -20°C until used. CM (200 µL) was assayed for VEGF concentration according the manufacturer's instructions.

Analyses of post-ischemic blood flow recovery and muscular microvessel density in nude mice with limb ischemia

Immunocompromised CD1-*Foxn1*nu mice (Charles River, UK, n=11 to 14 mice/group) underwent unilateral limb ischemia as previously reported[10] and were immediately transplanted with engineered PACs in their ischemic adductor muscle. Post-ischemic foot blood flow recovery was measured at 30 minutes, 7 days and 14 days after ischemia by using a high resolution laser Doppler imaging system (MoorLDI2, Moor Instruments, Axminster, UK). At 14 days post-surgery, the limbs of terminally anesthetized mice were perfusion-fixed and ischemic adductor muscles harvested for histological analyses. Evaluation of capillary and arteriolar density was performed in transverse muscular sections

(5 μm thick) after fluorescent immunohistochemical staining for α-smooth muscle actin (α-SMA, Sigma) to identify muscularized blood vessels (and hence arterioles) and with fluorescent isolectin-B4 (Invitrogen), which binds to endothelial cells. High power fields were captured (at 200X) using a fluorescent microscope. Arterioles were recognized as vessels with one or more continuous layers of α-SMA-positive vascular smooth muscle cells and an isolectin-B4 positive lumen. According to their luminal diameter, arterioles were also stratified as ≤20 μm and ≤ 50μm. The number of capillaries per mm^2 was evaluated in the same sections by counting the number of isolectin-B4-positive and α-SMA-negative microvessels.

Supplemental References

1. Campagnolo P, Cesselli D, Al Haj Zen A, Beltrami AP, Krankel N, Katare R, Angelini G, Emanueli C, Madeddu P. Human adult vena saphena contains perivascular progenitor cells endowed with clonogenic and proangiogenic potential. *Circulation.* 2010;121:1735-1745.

2. Thery C, Amigorena S, Raposo G, Clayton A. Isolation and characterization of exosomes from cell culture supernatants and biological fluids. *Curr Protoc Cell Biol.* 2006;Chapter 3:Unit 3 22.

3. Sahoo S, Klychko E, Thorne T, Misener S, Schultz KM, Millay M, Ito A, Liu T, Kamide C, Agrawal H, Perlman H, Qin G, Kishore R, Losordo DW. Exosomes from human CD34(+) stem cells mediate their proangiogenic paracrine activity. *Circ Res.* 2011;109:724-728.

4. Kroh EM, Parkin RK, Mitchell PS, Tewari M. Analysis of circulating microRNA biomarkers in plasma and serum using quantitative reverse transcription-PCR (qRT-PCR). *Methods.* 2010;50:298-301.

5. Arroyo JD, Chevillet JR, Kroh EM, Ruf IK, Pritchard CC, Gibson DF, Mitchell PS, Bennett CF, Pogosova-Agadjanyan EL, Stirewalt DL, Tait JF, Tewari M. Argonaute2 complexes carry a population of circulating microRNAs independent of vesicles in human plasma. *Proc Natl Acad Sci U S A.* 2011;108:5003-5008.

6. Pfaffl MW. A new mathematical model for relative quantification in real-time RT-PCR. *Nucleic Acids Res.* 2001;29:e45.

7. Caporali A, Meloni M, Vollenkle C, Bonci D, Sala-Newby GB, Addis R, Spinetti G, Losa S, Masson R, Baker AH, Agami R, le Sage C, Condorelli G, Madeddu P, Martelli F, Emanueli C. Deregulation of microRNA-503 contributes to diabetes mellitus-induced impairment of endothelial function and reparative angiogenesis after limb ischemia. *Circulation.* 2011;123:282-291.

8. Pfaffl MW. A-Z of quantitative PCR. Quantification strategies in real-time PCR *International University Line (IUL), La Jolla, CA, USA.*Chapter 3:.

9. Bustin SA. Absolute quantification of mRNA using real-time reverse transcription polymerase chain reaction assays. *J Mol Endocrinol.* 2000;25:169-193.

10. Kane NM, Meloni M, Spencer HL, Craig MA, Strehl R, Milligan G, Houslay MD, Mountford JC, Emanueli C, Baker AH. Derivation of Endothelial Cells From Human Embryonic Stem Cells by Directed Differentiation: Analysis of MicroRNA and Angiogenesis In Vitro and In Vivo. *Arterioscler Thromb Vasc Biol.* 2010;30:1389-1397.

11. He B, Xiao J, Ren AJ, Zhang YF, Zhang H, Chen M, Xie B, Gao XG, Wang YW. Role of miR-1 and miR-133a in myocardial ischemic postconditioning. *J Biomed Sci.* 2011;18:22.

12. Elia L, Contu R, Quintavalle M, Varrone F, Chimenti C, Russo MA, Cimino V, De Marinis L, Frustaci A, Catalucci D, Condorelli G. Reciprocal Regulation of MicroRNA-1 and Insulin-Like Growth Factor-1 Signal Transduction Cascade in Cardiac and Skeletal Muscle in Physiological and Pathological Conditions. *Circulation.* 2009;120:2377-2385.

13. Duan X, Ji B, Wang X, Liu J, Zheng Z, Long C, Tang Y, Hu S. Expression of MicroRNA-1 and MicroRNA-21 in Different Protocols of Ischemic Conditioning in an Isolated Rat Heart Model. *Cardiology.* 2012;122:36-43.

14. Zhang H, Qi M, Li S, Qi T, Mei H, Huang K, Zheng L, Tong Q. microRNA-9 Targets Matrix Metalloproteinase 14 to Inhibit Invasion, Metastasis, and Angiogenesis of Neuroblastoma Cells. *Molecular Cancer Therapeutics.* 2011;11:1454-1466.

15. Zhuang G, Wu X, Jiang Z, Kasman I, Yao J, Guan Y, Oeh J, Modrusan Z, Bais C, Sampath D, Ferrara N. Tumour-secreted miR-9 promotes endothelial cell migration and angiogenesis by activating the JAK-STAT pathway. *EMBO J.* 2012.

16. Bonci D, Coppola V, Musumeci M, Addario A, Giuffrida R, Memeo L, D'Urso L, Pagliuca A, Biffoni M, Labbaye C, Bartucci M, Muto G, Peschle C, De Maria R. The miR-15a-miR-16-1 cluster controls prostate cancer by targeting multiple oncogenic activities. *Nat Med.* 2008;14:1271-1277.

17. Yin KJ, Olsen K, Hamblin M, Zhang J, Schwendeman SP, Chen YE. Vascular endothelial cell-specific microRNA-15a inhibits angiogenesis in hindlimb ischemia. *J Biol Chem.* 2012.

18. Caporali A, Emanueli C. MicroRNA-503 and the Extended MicroRNA-16 Family in Angiogenesis. *Trends in Cardiovascular Medicine* 2012;21:162-166.

19. Finnerty JR, Wang WX, Hebert SS, Wilfred BR, Mao G, Nelson PT. The miR-15/107 group of microRNA genes: evolutionary biology, cellular functions, and roles in human diseases. *J Mol Biol.* 2012;402:491-509.

20. Liu Z, Yang D, Xie P, Ren G, Sun G, Zeng X, Sun X. MiR-106b and MiR-15b Modulate Apoptosis and Angiogenesis in Myocardial Infarction. *Cell Physiol Biochem.* 2012;29:851-862.

21. Hullinger TG, Montgomery RL, Seto AG, Dickinson BA, Semus HM, Lynch JM, Dalby CM, Robinson K, Stack C, Latimer PA, Hare JM, Olson EN, van Rooij E. Inhibition of miR-15 protects against cardiac ischemic injury. *Circ Res.* 2012;110(1):71-81.

22. Chamorro-Jorganes A, Araldi E, Penalva LO, Sandhu D, Fernandez-Hernando C, Suarez Y. MicroRNA-16 and microRNA-424 regulate cell-autonomous angiogenic functions in endothelial cells via targeting vascular endothelial growth factor receptor-2 and fibroblast growth factor receptor-1. *Arterioscler Thromb Vasc Biol.* 2011;31:2595-2606.

23. Poliseno L, Tuccoli A, Mariani L, Evangelista M, Citti L, Woods K, Mercatanti A, Hammond S, Rainaldi G. MicroRNAs modulate the angiogenic properties of HUVECs. *Blood.* 2006;108:3068-3071.

24. Dews M, Homayouni A, Yu D, Murphy D, Sevignani C, Wentzel E, Furth EE, Lee WM, Enders GH, Mendell JT, Thomas-Tikhonenko A. Augmentation of tumor angiogenesis by a Myc-activated microRNA cluster. *Nat Genet.* 2006;38:1060-1065.

25. Otsuka M, Zheng M, Hayashi M, Lee J-D, Yoshino O, Lin S, Han J. Impaired microRNA processing causes corpus luteum insufficiency and infertility in mice. *The Journal of Clinical Investigation.* 2008;118:1944-1954.

26. Suarez Y, Fernandez-Hernando C, Yu J, Gerber SA, Harrison KD, Pober JS, Iruela-Arispe ML, Merkenschlager M, Sessa WC. Dicer-dependent endothelial microRNAs are necessary for postnatal angiogenesis. *Proc Natl Acad Sci U S A.* 2008;105:14082-14087.

27. Doebele C, Bonauer A, Fischer A, Scholz A, Reiss Y, Urbich C, Hofmann W-K, Zeiher AM, Dimmeler S. Members of the microRNA-17-92 cluster exhibit a cell-intrinsic antiangiogenic function in endothelial cells. *Blood.* 2010;115:4944-4950.

28. Yin R, Bao W, Xing Y, Xi T, Gou S. MiR-19b-1 inhibits angiogenesis by blocking cell cycle progression of endothelial cells. *Biochem Biophys Res Commun.* 2012;417:771-776.

29. Hua Z, Lv Q, Ye W, Wong CK, Cai G, Gu D, Ji Y, Zhao C, Wang J, Yang BB, Zhang Y. MiRNA-directed regulation of VEGF and other angiogenic factors under hypoxia. *PLoS One.* 2006;1:e116.

30. Larsson E, Fredlund Fuchs P, Heldin J, Barkefors I, Bondjers C, Genove G, Arrondel C, Gerwins P, Kurschat C, Schermer B, Benzing T, Harvey SJ, Kreuger J, Lindahl P. Discovery of microvascular miRNAs using public gene expression data: miR-145 is expressed in pericytes and is a regulator of Fli1. *Genome Med.* 2009;1:108.

31. Zhou Q, Gallagher R, Ufret-Vincenty R, Li X, Olson EN, Wang S. Regulation of angiogenesis and choroidal neovascularization by members of microRNA-23~27~24 clusters. *Proc Natl Acad Sci U S A.* 2011;108:8287-8292.

32. Fiedler J, Jazbutyte V, Kirchmaier BC, Gupta SK, Lorenzen J, Hartmann D, Galuppo P, Kneitz S, Pena JT, Sohn-Lee C, Loyer X, Soutschek J, Brand T, Tuschl T, Heineke J, Martin U, Schulte-Merker S, Ertl G, Engelhardt S, Bauersachs J, Thum T. MicroRNA-24 regulates vascularity after myocardial infarction. *Circulation.* 2011;124:720-730.

33. Urbich C, Kaluza D, Fromel T, Knau A, Bennewitz K, Boon RA, Bonauer A, Doebele C, Boeckel JN, Hergenreider E, Zeiher AM, Kroll J, Fleming I, Dimmeler S. MicroRNA-27a/b controls endothelial cell repulsion and angiogenesis by targeting semaphorin 6A. *Blood.* 2011;119:1607-1616.

34. Bonauer A, Carmona G, Iwasaki M, Mione M, Koyanagi M, Fischer A, Burchfield J, Fox H, Doebele C, Ohtani K, Chavakis E, Potente M, Tjwa M, Urbich C, Zeiher AM, Dimmeler S. MicroRNA-92a controls angiogenesis and functional recovery of ischemic tissues in mice. *Science.* 2009;324:1710-1713.

35. Zhang Q, Kandic I, Kutryk MJ. Dysregulation of angiogenesis-related microRNAs in endothelial progenitor cells from patients with coronary artery disease. *Biochemical and Biophysical Research Communications.* 2011;405:42-46.

36. Grundmann S, Hans FP, Kinniry S, Heinke J, Helbing T, Bluhm F, Sluijter JP, Hoefer I, Pasterkamp G, Bode C, Moser M. MicroRNA-100 regulates neovascularization by suppression of mammalian target of rapamycin in endothelial and vascular smooth muscle cells. *Circulation.* 2011;123:999-1009.

37. Trajkovski M, Hausser J, Soutschek J, Bhat B, Akin A, Zavolan M, Heim MH, Stoffel M. MicroRNAs 103 and 107 regulate insulin sensitivity. *Nature.* 2011;474(7353):649-653.

38. Feng L, Xie Y, Zhang H, Wu Y. miR-107 targets cyclin-dependent kinase 6 expression, induces cell cycle G1 arrest and inhibits invasion in gastric cancer cells. *Med Oncol.* 2012;29:856-863.

39. Fish JE, Santoro MM, Morton SU, Yu S, Yeh RF, Wythe JD, Ivey KN, Bruneau BG, Stainier DY, Srivastava D. miR-126 regulates angiogenic signaling and vascular integrity. *Dev Cell.* 2008;15:272-284.

40. Meng S, Cao JT, Zhang B, Zhou Q, Shen CX, Wang CQ. Downregulation of microRNA-126 in endothelial progenitor cells from diabetes patients, impairs their functional properties, via target gene Spred-1. *Journal of Molecular and Cellular Cardiology.* 2012;53:64-72.

41. Chen Y, Gorski DH. Regulation of angiogenesis through a microRNA (miR-130a) that down-regulates antiangiogenic homeobox genes GAX and HOXA5. *Blood.* 2008;111:1217-1226.

42. Anand S, Majeti BK, Acevedo LM, Murphy EA, Mukthavaram R, Scheppke L, Huang M, Shields DJ, Lindquist JN, Lapinski PE, King PD, Weis SM, Cheresh DA. MicroRNA-132-mediated loss of p120RasGAP activates the endothelium to facilitate pathological angiogenesis. *Nat Med.* 2010;16:909-914.

43. Katare R, Riu F, Mitchell K, Gubernator M, Campagnolo P, Cui Y, Fortunato O, Avolio E, Cesselli D, Beltrami AP, Angelini G, Emanueli C, Madeddu P. Transplantation of human pericyte progenitor cells improves the repair of infarcted heart through activation of an angiogenic program involving micro-RNA-132. *Circ Res.* 2011;109:894-906.

44. Ott CE, Grunhagen J, Jager M, Horbelt D, Schwill S, Kallenbach K, Guo G, Manke T, Knaus P, Mundlos S, Robinson PN. MicroRNAs differentially expressed in postnatal

aortic development downregulate elastin via 3' UTR and coding-sequence binding sites. *PLoS One.* 2011;6:e16250.

45. Porrello ER, Johnson BA, Aurora AB, Simpson E, Nam YJ, Matkovich SJ, Dorn GW, 2nd, van Rooij E, Olson EN. MiR-15 family regulates postnatal mitotic arrest of cardiomyocytes. *Circ Res.* 2011;109:670-679.

46. Kuehbacher A, Urbich C, Zeiher AM, Dimmeler S. Role of Dicer and Drosha for endothelial microRNA expression and angiogenesis. *Circ Res.* 2007;101:59-68.

47. Wurdinger T, Tannous BA, Saydam O, Skog J, Grau S, Soutschek J, Weissleder R, Breakefield XO, Krichevsky AM. miR-296 regulates growth factor receptor overexpression in angiogenic endothelial cells. *Cancer Cell.* 2008;14:382-393.

48. Lee Y, Kim M, Han J, Yeom KH, Lee S, Baek SH, Kim VN. MicroRNA genes are transcribed by RNA polymerase II. *EMBO J.* 2004;23:4051-4060.

49. Nakashima T, Jinnin M, Etoh T, Fukushima S, Masuguchi S, Maruo K, Inoue Y, Ishihara T, Ihn H. Down-regulation of mir-424 contributes to the abnormal angiogenesis via MEK1 and cyclin E1 in senile hemangioma: its implications to therapy. *PLoS One.* 2010;5:e14334.

Online Table I. Characteristics of the human populations who donated their blood for this study

	Controls	CLI	T2D+CLI	
	N=43	N=20	N=122	p-value
Age (years)	36.7 (7.3)	77.7 (9.7)	71.2 (9.3)	<0.0001
Gender (% males)	38	60	67	0.01

Quantitative data are expressed as mean and standard deviation (SD).
CLI=critical limb ischemia, T2D= type2 diabetes

Online Table II. Characteristics of the healthy human sub-population who donated blood for testing the effect of engineered PACs in mice with limb ischemia

	Healthy Donors (n=10)
Age (years)	35.2 (8.9)
Gender (% males)	60

Quantitative data are expressed as mean and standard deviation (SD).

Online Table III. miR and angiogenesis: evidences supporting the selection of 28 miRs screened in human PACs

miR	Expressed by EC or EPC	miR-16 family membership	Target genes with angiogeneis regulation potential	Induced by angiogenesis stimuli or inhibitors	Ref
miR-1	YES		HSP60, HSP70, KLF4	Myocardial infarction Cardiac ischemia preconditioning	He et al. 2011[11], Elia et al. 2009[12], Kane et al. 2010[10], Duan et al 2012[13]
miR-9	YES		MMP-14		Zhang et al 2012[14], Zhuang et al 2012[15]
miR-15a	YES	YES	BCL-2, VEGF, FGF2	Cardiac ischemia	Bonci et al. 2008[16], Yin et al. 2012[17], Caporali et al. 2012[18], Finnerty et al. 2012[19]
miR-15b	YES	YES	Pdk4, Sgk1	Cardiac ischemia	Liu et al 2012[20], Hullinger et al. 2012[21], Caporali et al. 2012[18], Finnerty et al. 2012[19]
miR-16	YES	YES	VEGF, KDR, FGFR	VEGF, bFGF	Chamorro-Jorganes et al. 2011[22], Poliseno et al. 2006[23], Caporali et al. 2012[18], Finnerty et al. 2012[19]
miR-17	YES		Tsp-1, TIMP-1	VEGF	Dews et al. 2006[24],

				Otsuka et al. 2008[25], Suarez et al. 2008[26], Doebele et al. 2010[27]
miR-18a	YES		VEGF	Doebele et al. 2010[27], Suarez et al. 2008[26]
miR-19a	YES		ischemia	Doebele et al. 2010[27]
miR-19b	YES	FGFR2	ischemia	Yin et al. 2012[28], Doebele et al. 2010[27]
miR-20a	YES	VEGF	VEGF	Hua et al. 2006[29], Suarez et al 2008[26] Doebele et al. 2010[27]
miR-23a	YES	Sprouty/Sema 6A		Polisenso et al. 2006[23], Larsson et al. 2009[30], Zhou et al. 2011[31]
miR-24	YES	GATA2, PAK4	Cardiac ischemia	Polisenso et al. 2006[23], Larsson et al. 2009[30], Fiedler et al. 2011[32]
miR-27	YES	Sprouty/Sema 6A		Zhou et al. 2011[31], Urbich et al. 2011[33]
miR-92a	YES	ITGB5	Limb and cardiac ischemia	Bonauer et al. 2009[34], Zhang et al. 2011[35], Doebele et al. 2010[27]

miR-100	YES		mTOR	Limb ischemia	Grundmann et al. 2011[36]
miR-103	YES	YES	Caveolin-1	T2D	Polisenso et al. 2006[23], Trajkovski et al. 2011[37], Caporali et al. 2012[18], Finnerty et al. 2012[19]
miR-107	?	YES	CDK6, Caveolin-1	T2D	Feng et al. 2012[38], Trajkovski et al. 2011[37], Caporali et al. 2012[18], Finnerty et al. 2012[19]
miR-126	YES		Spred1/PIIG3 R2		Fish et al. 2008[39], Zhang et al. 2011[35], Meng et al 2012[40], Larsson et al. 2009[30]
miR-130a	YES		HOXA5, GAX	VEGF, bFGF	Zhang et al. 2011[35], Chen et al. 2008[41]
miR-132	YES			VEGF, bFGF	Anand et al. 2010[42] ,Katare et al 2011[43]
miR-195	?	YES	CDK4, ELN, Col1a1, Col1a2, Check1	Aortic and heart development	Ott et al. 2011[44], Porrello et al. 2011[45], Caporali et al. 2012[18], Finnerty et al. 2012[19]

miR-221	YES		c-kit		Polisenso et al[23]. 2006, Zhang et al. 2011[35], Kuehbach er et al. 2007[46]
miR-222	YES		c-kit		Polisenso et al[23]. 2006, Zhang et al. 2011[35], Kuehbach er et al. 2007[46]
miR-296	YES		HGF	VEGF, EGF	Wurdinger et al. 2008[47]
miR-378	YES		Sufu, Fus-1		Lee et al. 2004[48]
miR-424	YES	YES	VEGFR2, FGF-R1, VEGF, MEK, CCNE1	Hypoxia,Ischemia, Hemangioma, VEGFA, bFGF	Ghosh et al. 2010, Chamorro-Jorganes et al. 2011[22], Nakashima et al. 2010[49], Caporali et al. 2012[18], Finnerty et al. 2012[19]
miR-497	?	YES	ELN, Col1a1, Col1a2	Aortic development	Ott et al. 2011[44], Caporali et al. 2012[18], Finnerty et al. 2012[19]
miR-503	YES	YES	CCNE1, cdc25A	T2D+CLI	Caporali et al.2011[7], Caporali et al. 2012[18], Finnerty et al. 2012[19]

Online Table III. Age, gender and clinical characteristics of type-2 diabetic patients at the moment they underwent angioplasty for critical limb ischemia

	T2D+CLI (n=122)
Age (years)	71.2 (9.3)
Gender (% males)	67
CAD (%)	48
Hypertension (%)	65
Neuropathy (%)	21
Retinopathy (%)	20
Ictus (%)	12
Active smoker (%)	13
HbA1c (%Hb)	7.8±1.5
Oral anti-diabetic drugs (%)	36
Insulin therapy (%)	64
Diet (%)	22
Aspirin therapy (%)	67
Clopidogrel therapy (%)	7
Anticoagulant therapy (%)	20
Statin therapy (%)	41

Quantitative data are expressed as mean and standard deviation (SD).
T2D= type2 diabetes, CLI=critical limb ischemia, CAD=coronary artery disease.

Online Table IV. Incidence of adverse events at one year follow up after angioplasty in type 2 diabetic patients described in Online Table IV (Total patients: N=122).

	N (%)
Any event	61 (50%)
Death (only)	17
Restenosis (only)	20
Amputation (only)	2
Restenosis and death	8
Restenosis and amputation	13
Restenosis and amputation and death	1
No event	61 (50%)

Online Table V. Association between miR expression and adverse events (restenosis and amputation)

Event	miR (2-ddCT)	OR*	95% CI	P-value
Restenosis (first event)	circulating miR-15a	1.28	1.01-1.61	0.04
	circulating miR-16	0.96	0.73-1.26	0.75
	PAC miR-15a	1.26	0.72-2.19	0.42
	PAC miR-16	0.79	0.51-1.23	0.30
Restenosis plus amputation	circulating miR-15a	2.10	1.32-3.36	0.002
	circulating miR-16	2.07	1.17-3.63	0.012
	PAC miR-15a	1.74	0.70-4.30	0.229
	PAC miR-16	0.70	0.35-1.41	0.315

*for 1 unit increase in log2

Online Table VI. Primers for VEGFA and AKT3 mutation

AKT3 mut1 Forward: 5'-AGTCTAAGGTCTCATGCTGTatttaattCTGTCTTACT -3' Reverse: 5'-ACAGCATGAGACCTTAGACTGAGATACAAT-3'
AKT3mut2 Forward: 5'-AAGTGCTGCGATTATAGACGatttaatCTGCACCTGG-3' Reverse: 5'-CGTCTATAATCGCAGCACTTTGGGAGGCCGA-3'
VEGFAmut Forward: 5'-ATTCGCCATTTTATTTTTCTatttaattAATCACCGAG-3' Reverse: 5'-AGAAAAATAAAATGGCGAATCCAATTCCAA-3'

Supplemental Figures and Figure legends

Online Figure I.

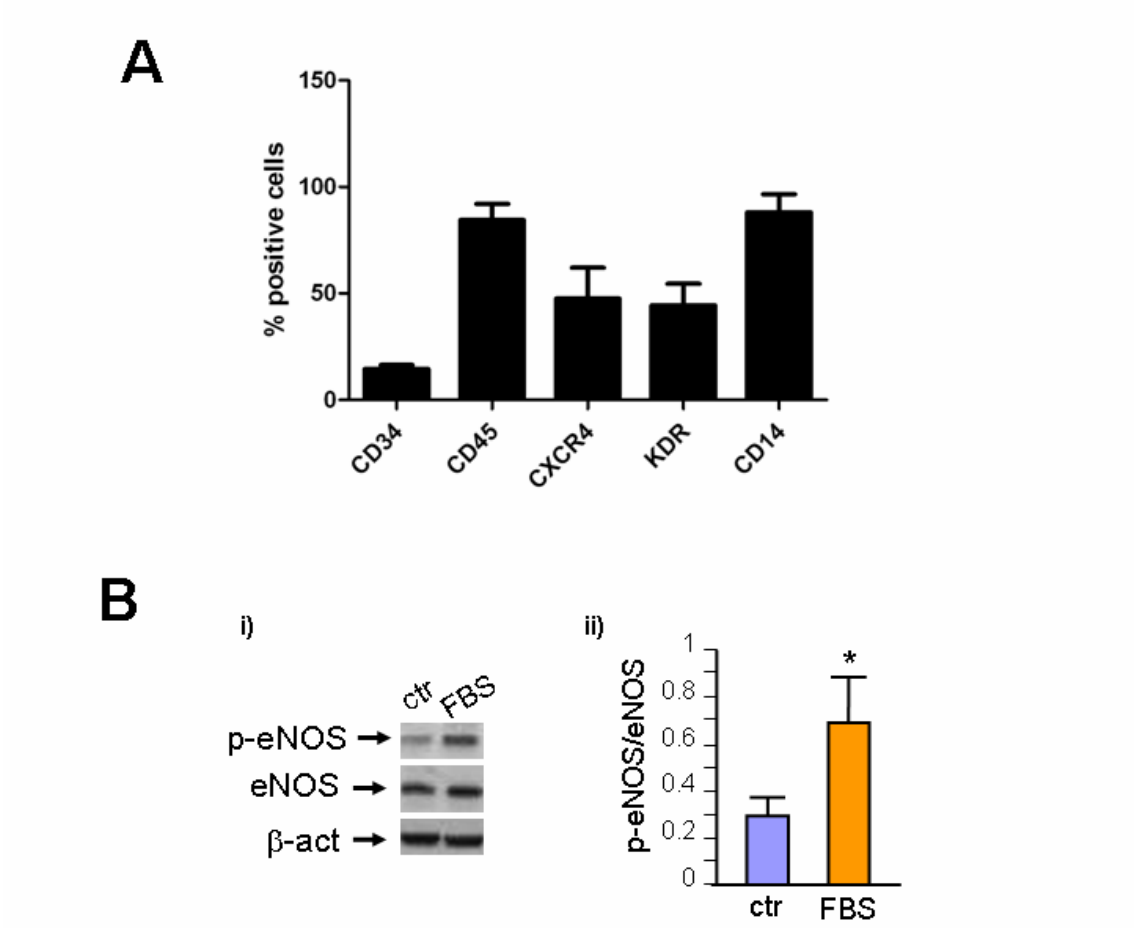

Online Figure I. Characterization of culture-selected PACs. A) Flow cytometric characterization of human PACs originated by culture selection from peripheral blood mononuclear cells (MNCs). Percentage cells positive for specific antigens are shown (n=8 donors). **B**) i) bar graph showing results of eNOS and phospho eNOS (p-eNOS) protein analysis by Western blot (n=3 PAC donor); ii) representative Western blot bands. All data are expressed as mean ±SEM.

Online Figure II.

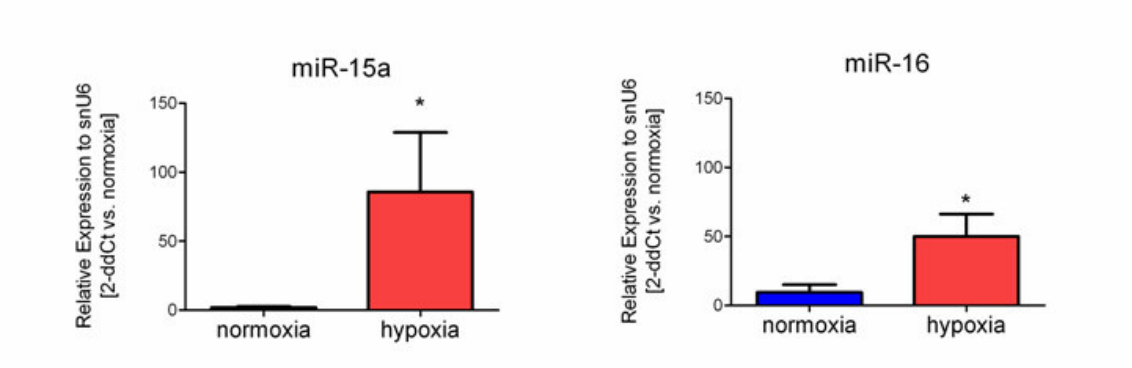

Online Figure II. Hypoxia increases miR-15a and miR-16 relative expression in healthy control PACs. PACs from healthy controls (n=10) were submitted to 48 hours hypoxia (2% oxygen) or kept under normal normoxic condition. miR-15a (left) and miR-16 (right) were measured by real time PCR using standard curves for miR-15a, miR-16 and Snu6. Data were normalized to snU6 and the relative expression of each of the two miR was quantified using the 2-ddCt method using as reference results obtained in PACs cultured in normoxia.. *p<0.05 vs. normoxia.

Online Figure III.

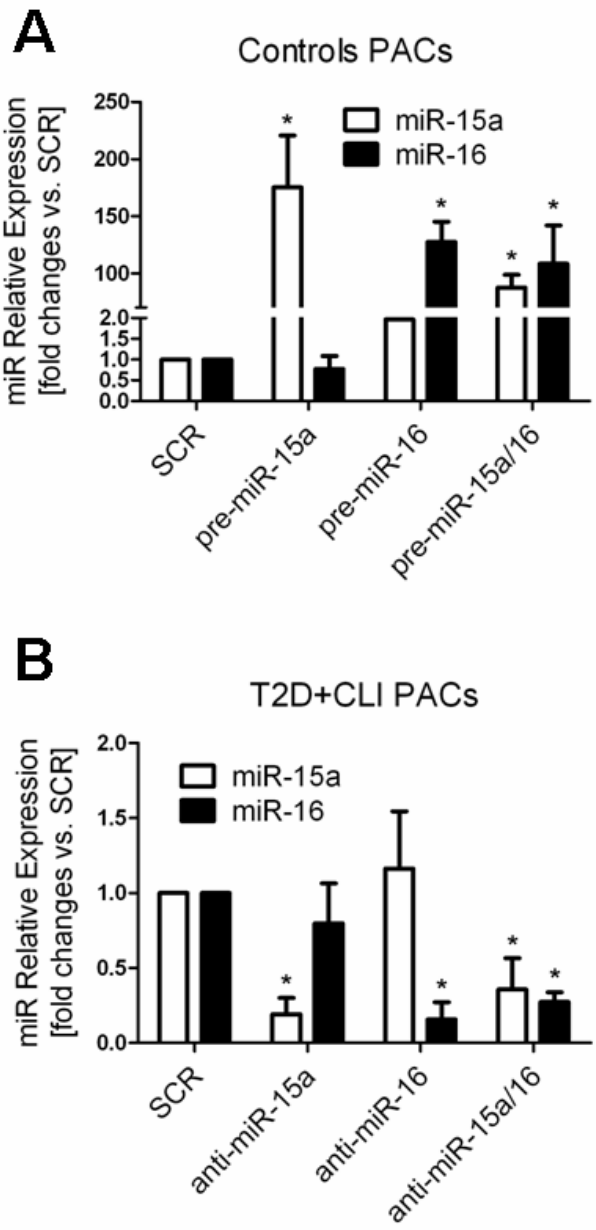

Online Figure III. miR-15a and miR-16 efficient expressional manipulation in human PACs. Relative expression (TaqMan PCR) of miR-15a and miR-16 after transfection with premiRs, antimiRs or scramble (SCR) control. **A**) Healthy (controls) PACs pre-miRs overexpression. **B**) T2D+CLI anti-miRs inhibition (both n=3 patients/group, *p<0.05 vs. SCR). All data are expressed as mean±SEM.

Online Figure IV.

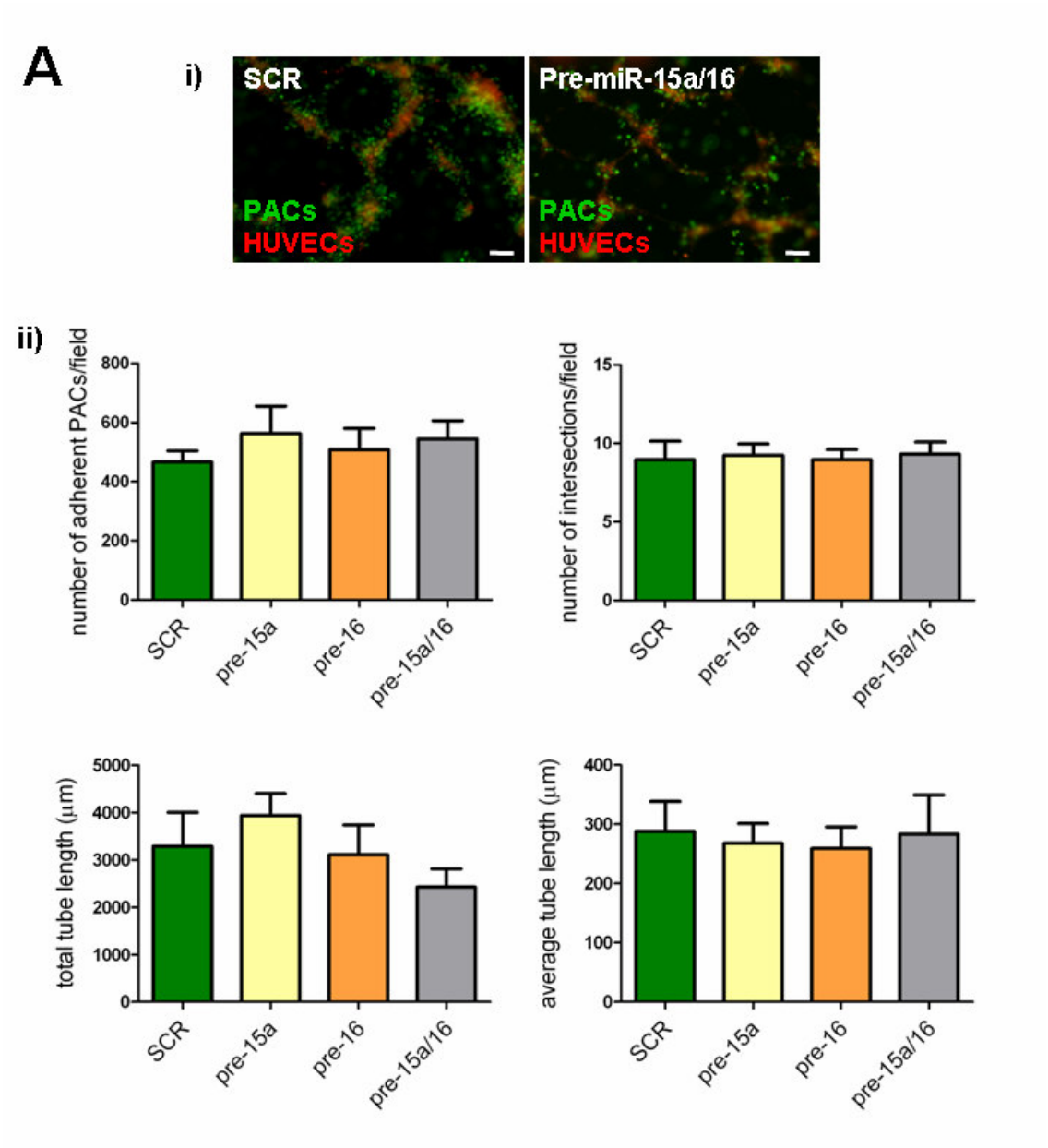

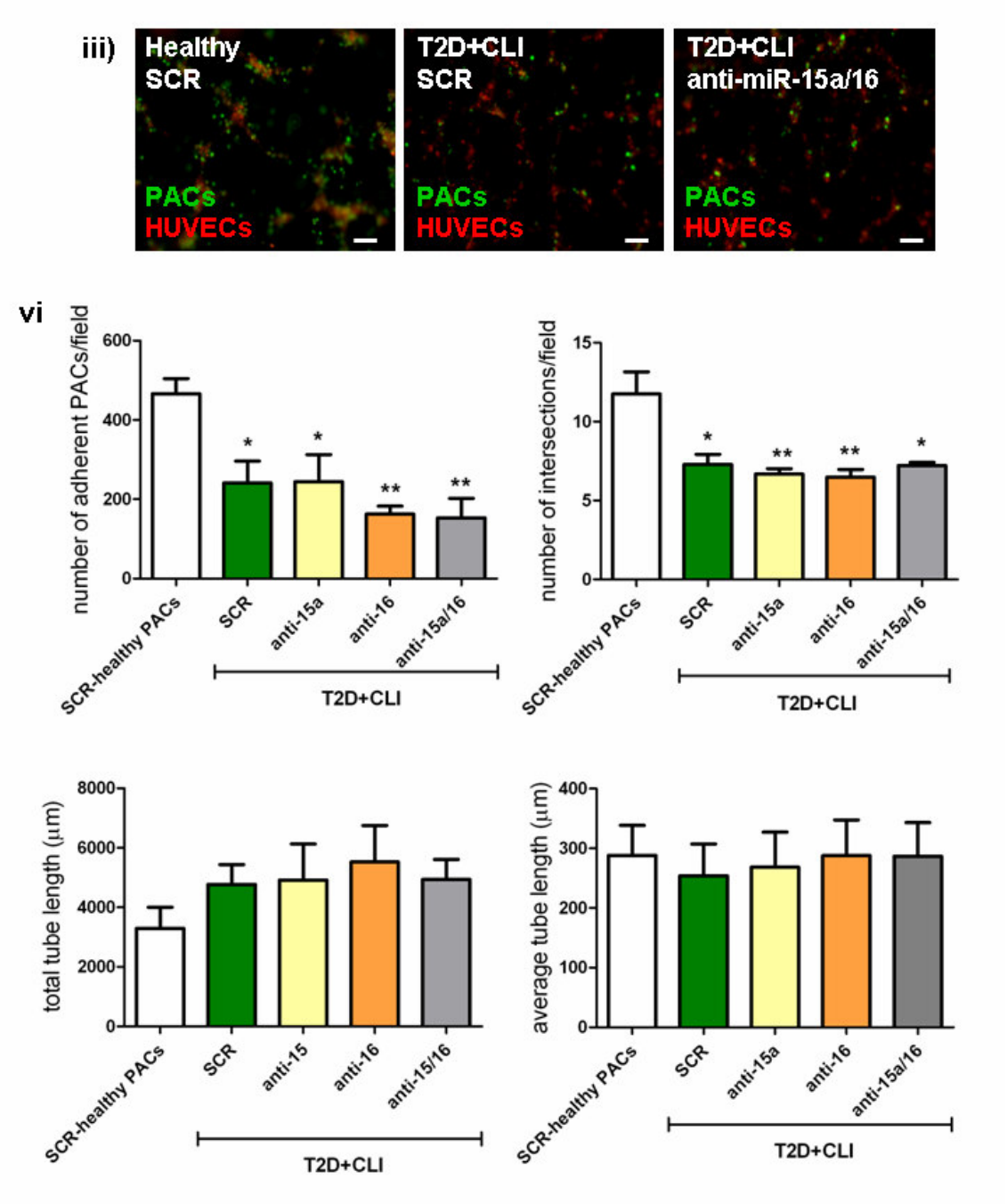

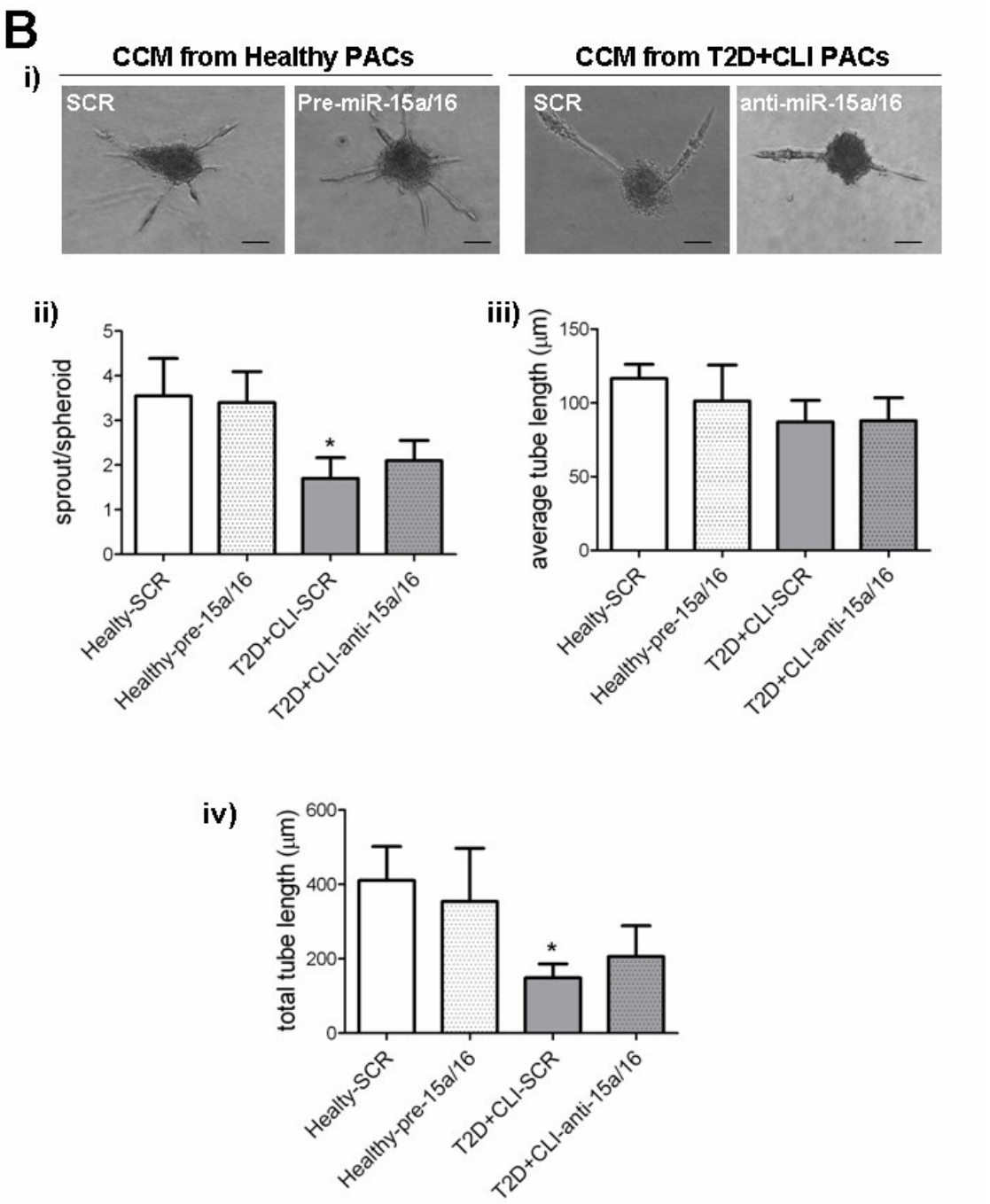

Online Figure IV. miR-15a/-16 manipulation in human PACs does not affect the ability of PACs to support EC networking. A) Capillary-like structure formation from HUVECs seeded on Matrigel and stimulated with: **i, ii**) control (healthy) PACs or **iii, iv**) T2D+CLI-PACs. Upper panels (**i, iii**): representative photomicrographs. Lower panels (**ii, iv**): bar graphs with data expressed as mean ±SEM (n=4 to n=10 subjects assayed in duplicate, p=NS). **B**) Spheroid assay using HUVECs and CCM of engineered PACs from healthy donors and from patients with CLI and T2D: (n=4 donors per group; each CCM was assayed in duplicate) i) representative photomicrographs, and measurements of ii) number of sprout per spheroid, iii) average tube length, and iv) total tube length. Data expressed as mean ±SEM. Scale bar: 100μm.

Online Figure V.

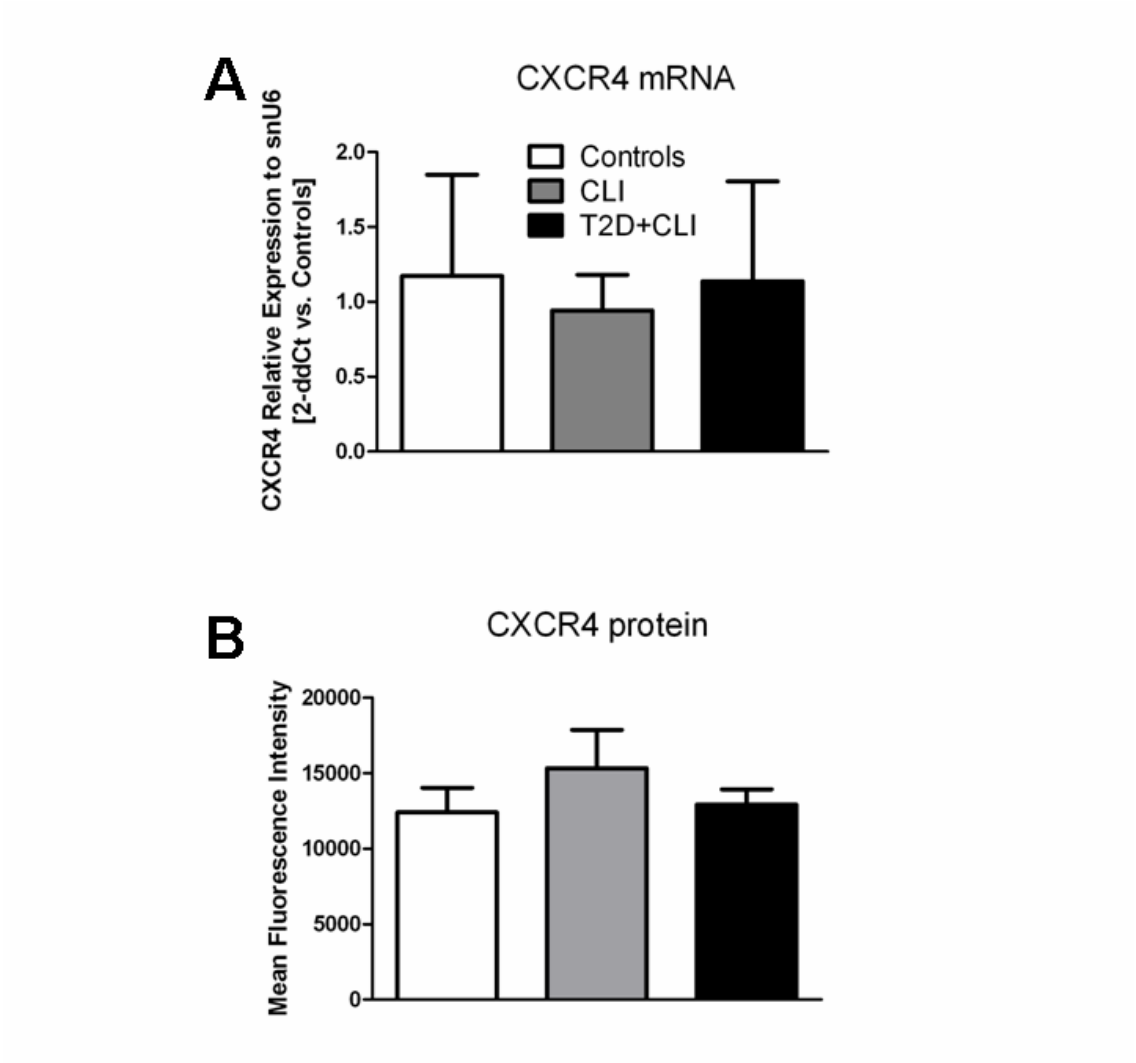

Online Figure V. CLI and diabetes do not induce CXCR4 expressional changes. Bar graphs showing CXCR4 expression: **A**) CXCR4 mRNA expression levels (TaqMan real time PCR) in PACs of the 3 groups of subjects enrolled to the study (n=6 subject per group); **B**) flowcytometric data of CXCR4 mean fluorescence intensity in circulating MNCs expressing PACs antigens ($CD34^{pos}/CD45^{dim}/CXCR4^{pos}/KDR^{pos}/CD14^{pos}$) is shown (controls: n=23, CLI: n=19, T2D+CLI: n=24). All data are expressed as mean±SEM.

Online Figure VI.

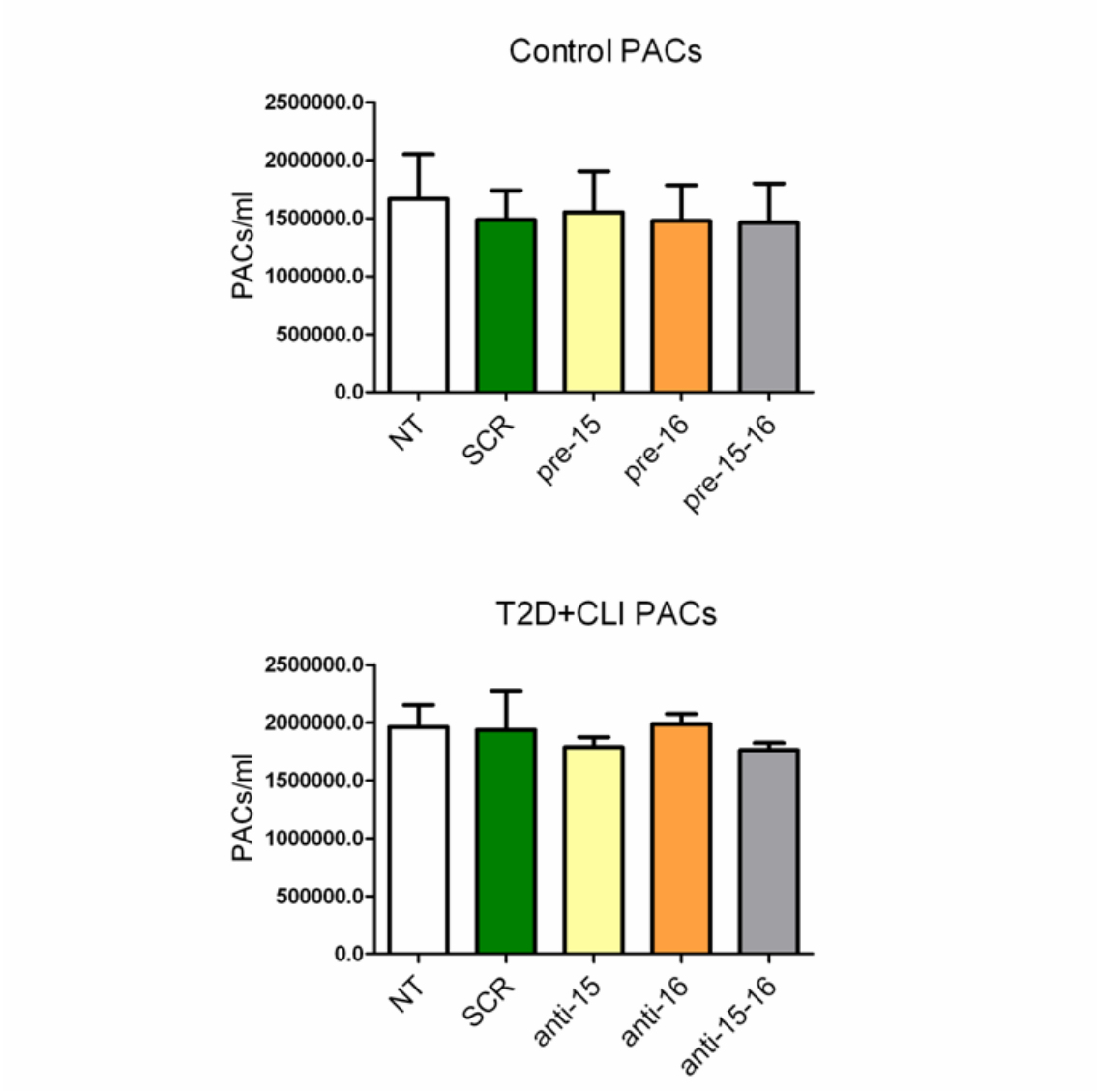

Online Figure VI. PACs cell number is not affected by either pre-miRs or anti-miRs for miR-15a or miR-16. Bar graph showing number of healthy control PACs (upper panel) or T2D+CLI-PACs (lower panel) after 48 hour transfection (n=3/group). Cell number was assayed by counting alive, trypan blue-negative PACs.

Online Figure VII.

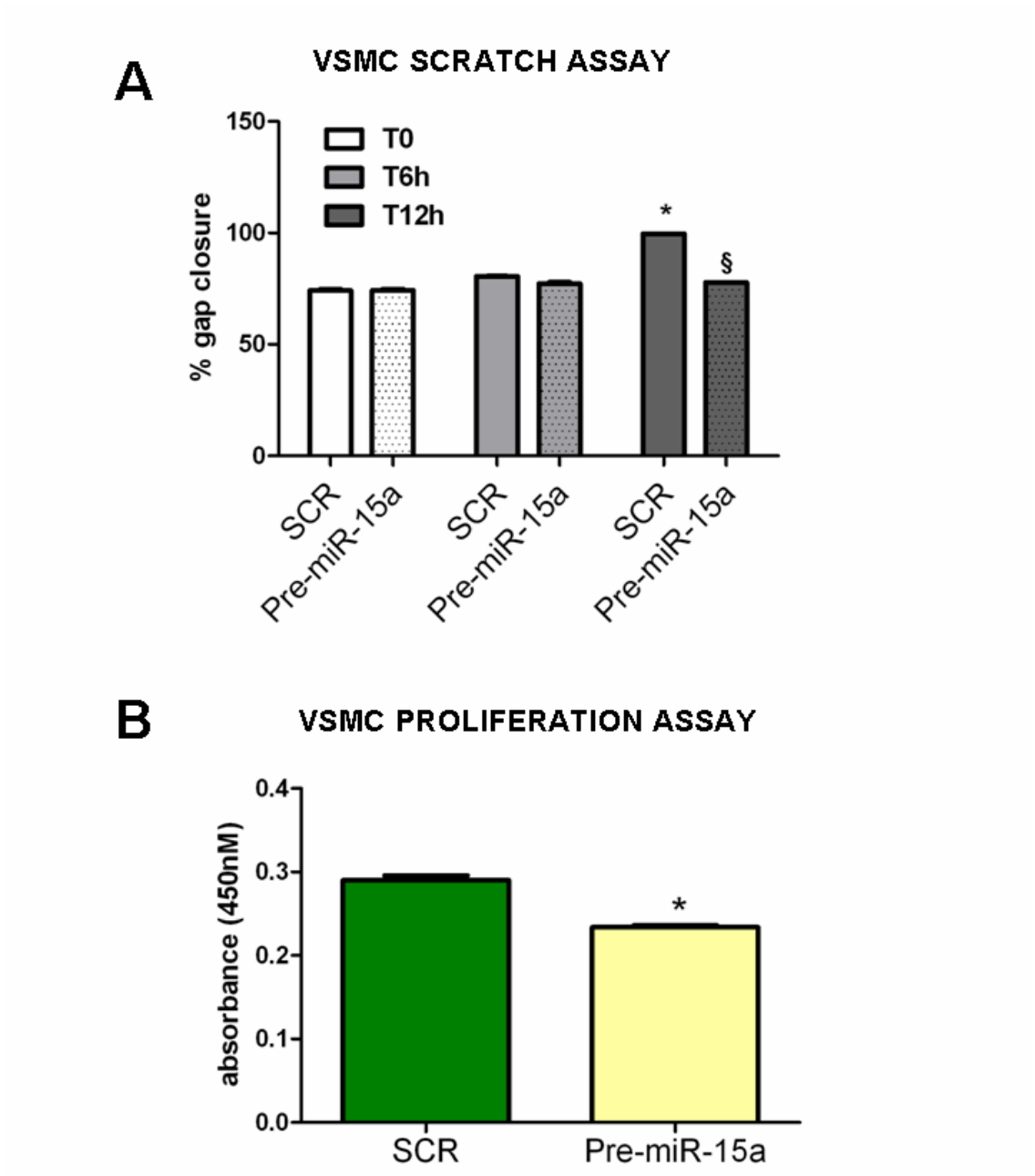

Online Figure VII. miR-15a overexpression negatively affects the ability human Vascular Smooth Muscle Cell (VSMC) to migrate and proliferate. A) VSMC migration was studied by scratch assay after 6 and 12 hours of scratching the cell monolayer. n=3 in quadruplicate, **p<0.001 vs. T0, §p<0.05 vs. SCR control. **B**) VSMC proliferation was assayed by BrDU incorporation, n=8 in quadruplicate, *p<0.05 vs. SCR control.